ACKNOWLEDGMENT

The author wishes to thank Y. Adelman, Supervisor of the project, for his time spent reviewing this paper and his associated comments, and R. Engelberg, his colleague, for also reviewing this paper.

REFERENCES

[1] J M. Cusack *et al*, "Automatic load contour mapping for microwave power transistors," *IEEE Trans. Microwave Theory Tech*, vol. MTT-22, pp. 1146–1152, Dec. 1974.
[2] Y. Takayama, "A new load-pull characterization method for microwave power transistors," in *Dig. IEEE 1976 Int Microwave Symp.*, pp. 218–220.
[3] R. B. Stancliff and D D Poulin, "Harmonic load pull," in *Dig. IEEE 1979 Int. Microwave Symp.*, pp. 185–187.
[4] H. Abe and Y. Aono, "11 GHz GaAs power MESFET load-pull measurements utilizing a new method for determining tuner y parameters," *IEEE Trans. Microwave Theory Tech.*, vol. MTT-27, pp 394–399, May 1979.
[5] D Poulin, "Load-pull measurement help you meet your match," *Microwaves*, pp 61–65, Nov. 1980.
[6] G P Bava *et al.*, "Active load techniques for load-pull characterization at microwave frequencies," *Electron. Lett*, vol. 18, pp. 178–180, 1982
[7] R. S. Tucker and P. D. Bradley, "Computer-aided error correction of large-signal load-pull measurements," *IEEE Trans Microwave Theory Tech*, vol. MTT-32, pp 296–300, Mar. 1984.
[8] N. Kuhn, "Simplified signal-flow-graph analysis," *Microwave J.*, pp. 59–66, Nov. 1963.
[9] "Automating the HP8410B microwave network analyzer," HP Appl. Note 221A, June 1980
[10] E. F. Da Silva and M. K. McPhun, "Calibration techniques for one-port measurements," *Microwave J.*, pp. 97–100, June 1978.

Latching Ferrite Quadrupole-Field Devices

YANSHENG XU

Abstract—**In this paper a brief survey of research and development on latching ferrite quadrupole-field devices in China is presented. Initially, theoretical analyses and some general rules for these kinds of devices are given. Some practical construction techniques and experimental results are also presented. Finally, many practical devices are described (e.g. reciprocal phase shifters with fast switching polarizations, reciprocal phase shifters with transverse magnetization, duplex phase shifters). In general, latching ferrite quadrupole-field devices have many advantages, among them simplicity, ruggedness, and rapid switching.**

I. INTRODUCTION

Dual-mode ferrite devices have found widespread applications as polarizers, phase shifters, etc. In recent years the latching version of one of the most popular dual-mode devices—quadrupole-field ferrite devices—has been used in China [1], and theoretical and experimental work on them has been performed. Many new devices are constructed or are under development.

Manuscript received February 18, 1987; revised June 29, 1987
The author is with the Beijing Institute of Radio Measurement, P.O Box 3923, Beijing, China.
IEEE Log Number 8716595.

II. THEORY

Dual-mode ferrite devices are constructed in square or circular waveguides, and are usually analyzed by the coupled wave theory suggested by Schelkunoff more than 30 years ago [2]. First, we calculate the tensor permeability of ferrite, magnetized in an arbitrary direction. Generally speaking, the direction of magnetization changes from point to point, and at any point in space we use Cartesian coordinates (x, y, z) and allow the z axis to coincide with the direction of magnetization at this point. Then, we have

$$\begin{aligned} B_x &= \mu H_x - jkH_y \\ B_y &= jkH_x + \mu H_y \\ B_z &= \mu_z H_z . \end{aligned} \tag{1}$$

It is necessary to point out that the coordinates x, y, z in (1) change everywhere in space, and for simplicity we may write (1) as

$$\vec{B} = \mu\vec{H} + (\mu_z - \mu)(\vec{\gamma}\cdot\vec{H})\vec{\gamma} + jk\vec{\gamma}\times\vec{H} \tag{2}$$

where $\vec{\gamma}$ is the unit vector along the z axis (i.e., direction of magnetization at this point). In the calculation of dual-mode ferrite devices, the unit vector $\vec{\gamma}$ should be represented as the superposition of unit vectors of arbitrary orthogonal coordinates (u, v, w), used in our boundary value problem of electromagnetic theory:

$$\vec{\gamma} = \gamma_u\vec{u} + \gamma_v\vec{v} + \gamma_w\vec{w}$$

where $\vec{u}, \vec{v}, \vec{w}$ are unit vectors in the directions (u, v, w), and $\gamma_u, \gamma_v, \gamma_w$ are the projections of $\vec{\gamma}$ in the directions (u, v, w) respectively, and are functions of (u, v, w). From (2) we obtain the following tensor permeability in the coordinates (u, v, w):

$$\|\mu\| = \begin{bmatrix} \mu & -jk\gamma_w & jk\gamma_v \\ jk\gamma_w & \mu & -jk\gamma_u \\ -jk\gamma_v & jk\gamma_u & \mu \end{bmatrix} + (\mu_z - \mu)\begin{bmatrix} \gamma_u^2 & \gamma_u\gamma_v & \gamma_u\gamma_w \\ \gamma_u\gamma_v & \gamma_v^2 & \gamma_v\gamma_w \\ \gamma_u\gamma_w & \gamma_v\gamma_w & \gamma_w^2 \end{bmatrix}. \tag{3}$$

For weakly magnetized ferrites $\mu_z \approx \mu$ and

$$\|\mu\| = \begin{bmatrix} \mu & -jk\gamma_w & jk\gamma_v \\ jk\gamma_w & \mu & -jk\gamma_u \\ -jk\gamma_v & jk\gamma_u & \mu \end{bmatrix}. \tag{4}$$

Although (3) and (4) have already been obtained in other forms by coordinate transformations in the literature [3], this equation is very convenient and useful in calculating dual-mode ferrite devices, as shown in the following.

From Schelkunoff [2], we may expand the electromagnetic fields in waveguides containing transversely magnetized ferrites as the superposition of normal modes of electromagnetic waves in the empty waveguide (in the following, coordinate z coincides

with the axis of our waveguide):

$$E_u = \sum_n \left(V_n \frac{\partial \Pi_n}{e_1 \partial u} + V_n^* \frac{\partial \Pi_n^*}{e_2 \partial v} \right)$$

$$E_v = \sum_n \left(V_n \frac{\partial \Pi_n}{e_2 \partial v} - V_n^* \frac{\partial \Pi_n^*}{e_1 \partial u} \right)$$

$$H_u = \sum_n \left(- I_n \frac{\partial \Pi_n}{e_2 \partial V} + I_n^* \frac{\partial \Pi_n^*}{e_1 \partial u} \right)$$

$$H_v = \sum_n \left(I_n \frac{\partial \Pi_n}{e_1 \partial u} + I_n^* \frac{\partial \Pi_n^*}{e_2 \partial v} \right)$$

$$E_z = \sum_n X_n V_{z,n} \Pi_n$$

$$H_z = \sum_n X_n^* I_{z,n} \Pi_n^* \tag{5}$$

where Π_n and Π_n^* are Hertzian functions of the electromagnetic waves in the empty waveguide; e_1 and e_2 are the scale coefficients; V_n, V_n^*, I_n, I_n^*, $V_{z,n}$, and $I_{z,n}$ are coefficients of expansion and are functions of coordinate z only; and

$$\nabla_t^2 \Pi_n = - X_n^2 \Pi_n \qquad \nabla_t^2 \Pi_n^* = - X_n^{*2} \Pi_n^*.$$

Substituting (4) and (5) into Maxwell's equations, we have

$$\frac{dV_m}{dz} = \sum_n - \left(Z_{mn} I_n + Z_{mn^*} I_n^* + {}^V T_{mn} V_n + {}^V T_{mn^*} V_n^* \right)$$

$$\frac{dI_m}{dz} = \sum_n - \left(Y_{mn} V_n + Y_{mn^*} V_n^* + {}^I T_{mn} I_n + {}^I T_{mn^*} I_n^* \right)$$

$$\frac{dV_m^*}{dz} = \sum_n - \left(Z_{m^*n^*} I_n^* + Z_{m^*n} I_n + {}^V T_{m^*n^*} V_n^* + {}^V T_{m^*n} V_n \right)$$

$$\frac{dI_m^*}{dz} = \sum_n - \left(Y_{m^*n^*} V_n^* + Y_{m^*n} V_n + {}^I T_{m^*n^*} I_n^* + {}^I T_{m^*n} I_n \right) \tag{6}$$

and the coefficients Z, Y, and T can readily be obtained [see 2, eqs. (30), (39)–(44)].

The most important terms in (6) are those which contain the first power of k, i.e., the voltage transfer coefficients ${}^V T$ and current transfer coefficients ${}^I T$:

$${}^V T_{mn^*} = {}^I T_{n^*m} = \frac{jkX_n^{*2}}{\mu} \int_s \left(\gamma_v \Pi_n^* \frac{\partial \Pi_m}{e_2 \partial v} + \gamma_u \Pi_n^* \frac{\partial \Pi_m}{e_1 \partial u} \right) ds,$$

$${}^V T_{mn} = {}^I T_{mn} = 0$$

$${}^V T_{m^*n^*} = {}^I T_{n^*m^*} = \frac{jkX_n^{*2}}{\mu} \int_s \left(- \gamma_v \Pi_n^* \frac{\partial \Pi_m^*}{e_1 \partial u} + \gamma_u \Pi_n^* \frac{\partial \Pi_m^*}{e_2 \partial v} \right) ds,$$

$${}^V T_{n^*m} = {}^I T_{nm^*} = 0. \tag{7}$$

In cylindrical coordinates $u = r$, $v = \theta$, and from $\nabla \cdot \vec{B}_0 = 0$ ($\vec{B}_0$ is the magnetic induction of a static magnetizing field) we have two kinds of magnetization:

$$B_{0r} \sim \gamma_r \sim \cos n\theta \qquad B_{0\theta} \sim \gamma_\theta \sim \sin n\theta \tag{I}$$

or

$$B_{0r} \sim \gamma_r \sim \sin n\theta \qquad B_{0\theta} \sim \gamma_\theta \sim \cos n\theta. \tag{II}$$

And there are two sets of orthogonal modes in circular waveguides:

$$\Pi_k^* \sim \sum_n f_n^{\mathrm{I}}(r) \cos n\theta \qquad \Pi_k \sim \sum_n f_n^{\mathrm{II}}(r) \sin n\theta$$

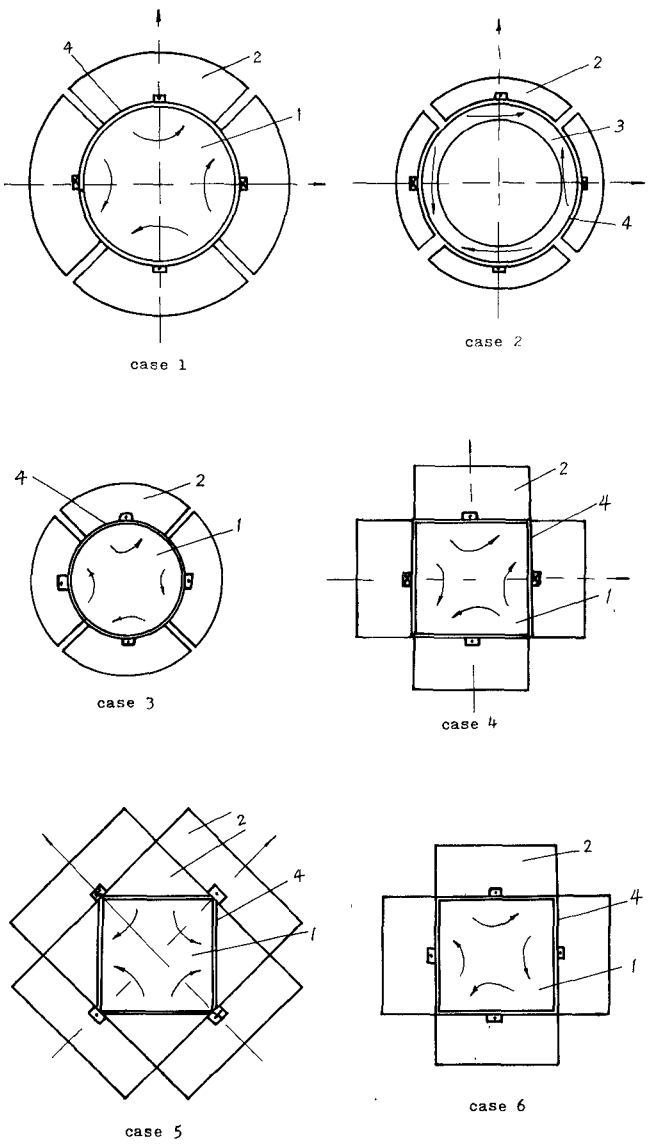

Fig. 1 Six cases of practical constructions: 1-ferrite rod, 2-magnetic yoke, 3-ferrite tube, 4-waveguide. Arrows in the waveguides show the directions of magnetization; arrows outside the waveguides show the directions of polarization of orthogonal modes.

and

$$\Pi_l^* \sim \sum_n f_n^{\mathrm{III}}(r) \sin n\theta \qquad \Pi_l \sim \sum_n f_n^{\mathrm{IV}}(r) \cos n\theta.$$

From (7) it is clear that only when the magnetization takes the form (II) are the transfer coefficients ${}^V T$ and ${}^I T$ all zero for the above two sets of eigenmodes, and are not coupled to each other. With square waveguides, the various modes may be considered as a superposition of cylindrical wave modes, and the above rule about eigenmodes may also be applied. In Fig. 1 some practical cases are given and the various polarizations of orthogonal eigenmodes are indicated by arrows. In the following, some practical constructions are presented and they are used to realize latching ferrite devices of practical interest.

III. Constructions of Practical Interest

There are six kinds of construction which find applications in practice (see Fig. 1). Of these, cases 3 and 6 are not quadrupole-field devices; they are used to construct polarization-insensitive

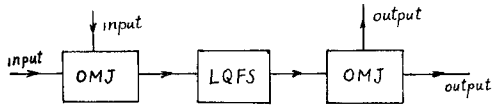

Fig. 2. Schematic diagram of latching variable power dividers or switches: OMJ-orthogonal mode junction; LQFS-latching quadrupole-field section.

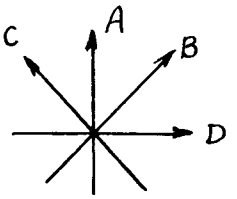

Fig. 3 Directions of polarization and principal axes of Fig. 2. A,D-directions of polarizations of input and output waves of OMJ; B,C-two principal axes of LQFS

phase shifters, but their construction is similar to the other four cases and hence we list them here also. Cases 1 and 2 are constructed in circular waveguides, the only difference between them being that in case 2 a ferrite tube instead of a ferrite rod is used to enhance the power capacity. The wall thickness of the ferrite tube is thinner, heat conduction is facilitated, the power concentration is less, and hence the peak power capacity is improved. On the other hand, the phase shift between the two orthogonal eigenmodes in case 2 is significantly less than in case 1 since the ferrite tube is essentially magnetized azimuthally and there are no circularly polarized components of the microwave magnetic field near the waveguide wall. Cases 5 and 4 are constructed in square waveguides and their magnetic yokes are also shown there. The difference of propagation constants of two orthogonal modes are (a and b being the dimensions of the waveguides):

case 1: $2.1\,(k/\mu)/a$

case 2: $6.22(k/\mu)[J_1(1.84) - J_1(1.84b/a)]/a,$
$(a-b)/a \ll 1$

case 4: $2.96(k/\mu)/a$

case 5: $4.3(k/\mu)/a$

case 6: $1.6(k/\mu)/a$

case 3 and 6: any polarization for two different directions of magnetization.

IV. Practical Devices Consisting of Latching Quadrupole-Field Sections

By combining latching quadrupole-field sections with other microwave components, many practical ferrite devices may be constructed. Some examples of them are described in the following.

1) Latching Variable Power Dividers or Switches: By combining two orthogonal mode junctions with one quadrupole-field section, a latching variable power divider can be constructed (see Fig. 2). In Fig. 3 the directions of polarization of the input and output waves and the two principal axes of the latching quadrupole-field section (QFS) are shown.

2) Reciprocal Phase Shifter with Fast Switching Polarizations: The schematic diagram is shown in Fig. 4. One of the fixed nonreciprocal polarizers (fixed $\lambda/4$ section) is replaced by a latching QFS ($\lambda/4$ section or other), and the polarizations of the output and received waves can be switched very quickly (several microseconds).

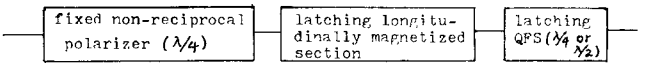

Fig. 4 Schematic diagram of reciprocal phase shifter with fast switching polarization.

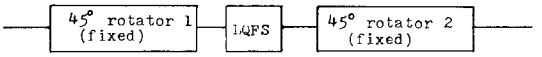

Fig. 5. Schematic diagram of latching reciprocal phase shifter with transverse magnetization.

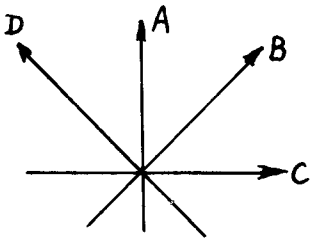

Fig. 6. Directions of polarization in Fig. 5. For propagation from left to right: A-polarization of input and output waves; B-polarization of output wave of 45° rotator 1; B,D-principal axes of LQFS.

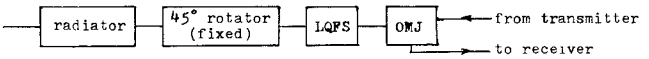

Fig. 7. Schematic diagram of duplexer-reciprocal phase shifter modules.

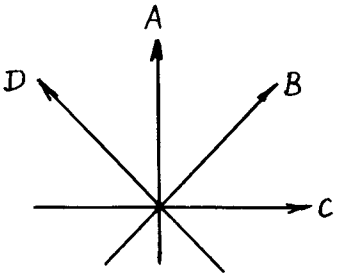

Fig 8. Directions of polarizations in Fig. 7. A-direction of polarization of radiator; B,D-principal axes of LQFS; B-polarization of wave to receiver; D-polarization of wave from transmitter.

3) Latching Reciprocal Phase Shifter with Transverse Magnetization: The schematic diagram is shown in Fig. 5 and the direction of polarization of the input and output waves and the principal axes of the latching QFS (LQFS) are shown in Fig. 6. This construction has a faster switching speed than the commonly used dual-mode reciprocal phase shifter.

4) Duplexer-Reciprocal Phase Shifter Modules: The schematic diagram is shown in Fig. 7. The direction of polarization and principal axes of the LQFS are shown in Fig. 8.

V. Experimental Results

Experimental results have been obtained from the practical devices that have been constructed [1], [4]–[6]. In the S-band, we choose $a/\lambda = 0.22$ and a model of case 4 in Fig. 1 is realized. With the length of the polarizer equal to 0.22λ, we obtain circularly polarized waves at the output port of the polarizer. The switching time of this polarizer is approximately 20 μs. In the C-band, latching polarizers with linearly polarized input waves and four output polarizations (vertically and horizontally polarized, left and right circularly polarized waves) are constructed with the following performance: cross modulation < 20 dB, ellipticity < 1 dB, insertion loss < 0.54 dB/360°, switching time

< 8 μs. In the C-band, a high-power variable power divider–combiner is realized by using the construction of case 2 in Fig. 1 with the following performance: bandwidth = 10 percent, insertion loss < 0.6 dB, VSWR < 1.25, switching time < 20 μs, peak power = 500 kW, average power = 500 W, phase shift between two orthogossionnal modes of the quadrupole-field section = 90°, power division–combination ratio = 3 dB.

The above results show that experiments are in good agreement with theory, and some practical devices have been constructed with many advantages over devices with electromagnets and holding currents.

References

[1] Xu Yansheng, "Miniaturized microwave ferrite latching polarizers," *Acta Electron.*, vol. 7, no. 4, pp. 49–56, Dec. 1979 (in Chinese).

[2] S. A. Schelkunoff, "Generalized telegraphist's equations for waveguides," *Bell Syst. Tech. J.*, vol. 31, pp. 784–801, July 1952.

[3] P. Hlawiczka, *Gyrotropic Waveguides*. New York: Academic Press, 1981.

[4] Jiang Renepi, Wei Kezhu, and Li Shigen, "Coupling-wave theory on latching variable polarizers," *Acta Electron. Sinica*, vol. 11, no. 1, p. 66, Jan. 1983 (in Chinese).

[5] Wei Kezhu *et al.*, presented on 1985 National Microwave Conference (in Chinese).

[6] Xu Yansheng and Jiang Zhengchang, "Dual-mode latching ferrite devices," *Microwave J.*, vol. 29, no. 5, pp. 277–285, May 1986.

Generalized Lorentz Gauge and Boundary Conditions in Partially Dielectric-Loaded Cylindrical Waveguide

JEONG-SIK CHOI, DUK-IN CHOI, AND SOON-CHUL YANG

***Abstract*—A generalized Lorentz gauge condition for the set of Vlasov–Maxwell equations is introduced. The condition is applied to the free-electron-laser instability of a relativistic electron beam in a partially dielectric-loaded waveguide. For the dielectric-loaded system with the external wiggler magnetic field, the potential approach with the generalized Lorentz gauge rather than the field approach is shown to be more convenient in the self-consistent study of free-electron-laser instability. We also derive the boundary conditions for potentials to be satisfied at the vacuum–dielectric interface and show that they are equivalent to the B_θ and E_θ continuous conditions in the field approach. An example is discussed to illustrate the equivalence between the two approaches of potentials and fields.**

I. Introduction

The instabilities of electromagnetic waves in dielectric-loaded cylindrical waveguide have been the subject of a number of recent investigations. [1]–[3] These works make use of the fluid Maxwell description and neglect the radial effect of the relativistic electron beam. Using the Vlasov–Maxwell scheme, Uhm and Davidson [4], [5] investigated the properties of free-electron-laser instability in a relativistic electron beam, which has a finite radial profile, propagating through a cylindrical vacuum waveguide. In their problem of the vacuum-beam boundary conditions for the system with the external wiggler magnetic field, the perturbed potential rather than the field was used in the self-consistent calculations of current and charge densities. To formulate the problem self-consistently, the potential approach is more convenient and is used extensively. For the problem of partially dielectric-loaded waveguide extending the vacuum waveguide case, the boundary conditions of potential quantities at the vacuum–dielectric interface are required. In this study the boundary conditions of the scalar and vector potentials at the vacuum–dielectric interface in a dielectric-loaded cylindrical waveguide are presented. In our analysis, we make use of a generalized Lorentz gauge condition for the potentials. It is shown that the boundary conditions on potentials are equivalent to the boundary conditions on electromagnetic fields. In addition, we discuss characteristics of the eigenmode that propagates through a partially dielectric-loaded cylindrical waveguide using the derived new potential boundary conditions.

Manuscript received February 26, 1987; revised July 8, 1987.

J.-S. Choi and D.-I. Choi are with the Department of Physics, Korea Advanced Institute of Science and Technology, Chungryang, Seoul, Korea.

S.-C Yang is with the Department of Physics, Mokpo National College, Muan, Chonnam 580-41, Korea

IEEE Log Number 8716911.

II. Formulation

We consider a partially dielectric-loaded cylindrical waveguide with a grounded conducting wall. The permeability of the dielectric material differs from unity by only a few parts in 10^5; thus in the Maxwell equations the permeability is set as $\mu = 1$. The displacement vector $\boldsymbol{D}$ is related to $\boldsymbol{E}$ as $\boldsymbol{D} = \epsilon \boldsymbol{E}$, where ϵ is the dielectric constant. Cylindrical coordinates (r, θ, z) are introduced and the dielectric constant is assumed to be only a function of the radial variable r.

In this analysis, a normal mode approach is adopted in which all quantities are assumed to vary according to

$$\Psi(x,t) = \hat{\Psi}(r)\exp[i(l\theta + kz - \omega t)] \tag{1}$$

where l is the azimuthal harmonic number, k is the axial wavenumber, ω is the eigenfrequency, and $\hat{\Psi}(r)$ is the amplitude. The scalar potential ϕ and the vector potential $\boldsymbol{A}$ are related to the fields $\boldsymbol{B}$ and $\boldsymbol{E}$ as

$$\boldsymbol{B} = \nabla \times \boldsymbol{A} \tag{2}$$

$$\boldsymbol{E} = -\nabla\phi - \frac{1}{c}\frac{\partial \boldsymbol{A}}{\partial t}. \tag{3}$$

Choosing the gauge condition

$$\nabla \cdot \boldsymbol{A} + \frac{\epsilon}{c}\frac{\partial \phi}{\partial t} = 0 \tag{4}$$

as the generalization of the Lorentz gauge to the case with dielectrics, the Maxwell equations for the potentials A_r, A_θ, A_z, and ϕ are given as

$$\left(\frac{1}{r}\frac{\partial}{\partial r}r\frac{\partial}{\partial r} - \frac{l^2}{r^2} + p^2\right)\hat{\phi}(r) + \frac{1}{\epsilon}\frac{d\epsilon}{dr}\frac{d\hat{\phi}}{dr} - \frac{i\omega}{\epsilon c}\frac{d\epsilon}{dr}\hat{A}_r(r) = 0 \tag{5}$$

$$\left(\frac{1}{r}\frac{\partial}{\partial r}r\frac{\partial}{\partial r} - \frac{l^2+1}{r^2} + p^2\right)\hat{A}_r(r) - \frac{2il}{r^2}\hat{A}_\theta(r) - \frac{i\omega}{c}\hat{\phi}(r)\frac{d\epsilon}{dr} = 0 \tag{6}$$

$$\left(\frac{1}{r}\frac{\partial}{\partial r}r\frac{\partial}{\partial r} - \frac{l^2+1}{r^2} + p^2\right)\hat{A}_\theta(r) + \frac{2il}{r^2}\hat{A}_r(r) = 0 \tag{7}$$

$$\left(\frac{1}{r}\frac{\partial}{\partial r}r\frac{\partial}{\partial r} - \frac{l^2}{r^2} + p^2\right)\hat{A}_z(r) = 0 \tag{8}$$

0018-9480/87/1100-1065$01.00 ©1987 IEEE